DOI: http://dx.doi.org/10.22104/ijhfc.2015.169

*Iranian Journal of Hydrogen & Fuel Cell 1(2015) 13-25*

Iranian Journal of Hydrogen & Fuel Cell

IJHFC

Journal homepage://ijhfc.irost.ir

# Investigation of ion transport and water content properties in anion exchange membranes based on polysulfone for solid alkaline fuel cell application

**Mona Iravaninia [1], Saba Azizi [1], Soosan Rowshanzamir [1,2,*]**

[1] School of Chemical Engineering, Iran University of Science and Technology, Narmak, Tehran 16846-13114, Iran
[2] Fuel Cell Laboratory, Green Research Centre, Iran University of Science and Technology, Tehran, Iran

**Article Information**

Article History:

Received:
13 July 2015
Received in revised form:
29 September 2015
Accepted:
03 October 2015

**Keywords**

Solid Alkaline Fuel Cell
Anion Exchange Membrane
Polysulfone
Amination Agents.

## Abstract

In the present research work, homogeneous anion exchange membranes based on polysulfone (QAPSFs) were prepared via chloromethylation, amination and alkalization. In the amination step, trimethylamine and N,N,N',N'-tetramethyl-1, 6-hexanediamine were used as amination and crosslinking agents, respectively. The chloromethylated polysulfone was characterized by $^1$HNMR spectroscopy and the chloromethylation degree was calculated using peak area integration. Ion transport properties, such as ionic conductivity, ion exchange capacity, and activation energy for hydroxide ion transport were measured for the prepared anion exchange membranes. Furthermore, water content associated properties, such water uptake and hydrated number, were determined for these membranes. According to the obtained results the membrane with crosslinking agent (QAPSF-2) showed ion transport properties quite similar to the membrane without the crosslinker (QAPSF-1). Although QAPSF-2 had more improved water content associated properties and reasonable dimensional stability in contrast to QAPSF-1. Finally, according to ionic transport measurements and water content characterizations, the prepared QAPSF membranes can be denoted as good candidates for solid alkaline fuel cell application.

## 1. Introduction

Fuel cells are known as promising technologies in the conversion of chemical energy into electrical energy due to high efficiency and low environmental impacts. In recent decade, solid alkaline fuel cells (SAFCs) or anion exchange membrane fuel cells (AEMFCs) have attracted more attention among different types of fuel cells. SAFCs are new technologies that utilize anion exchange membranes (AEMs) as solid polymer electrolytes. These types of fuel cells exhibit several advantages over proton exchange membrane fuel cells (PEMFCs) such as: minimizing corrosion problems under alkaline

---

[*] Corresponding Author's Tel.: Green Research Centre, Iran University of Science and Technology, Tehran, Iran. Tel.: +98 2177491223; fax: +98 217491242.
E-mail address: rowshanzamir@iust.ac.ir (S. Rowshanzamir).

media, employing less expensive metal catalysts (Ag, Ni, or Pd), effective reduction of oxygen in a cathode, using various liquid fuels and reducing fuel crossovering due to the opposite direction of fuel and hydroxide ion [1-4].

AEM is a key component of AEMFCs and has an important effect on the fuel cell performance. Different kinds of AEMs have been designed by changing the polymers chemistry, cationic groups and functionalization methods [5-15]. Among different polymers and cationic groups, polysulfone (PSF) and ammonium species are good candidates for AEM preparation [5, 11, 16-19]. PSF is a high performance engineering thermo plastic material in an amorphous glassy state with a glass transition temperature ($T_g$) of 195°C. This polymer is highly soluble in various polar solvents and shows good thermal, mechanical and chemical stability in different pH ranges [19, 20]. Quaternary ammonium (QA) groups are the most popular functional groups used in AEM fabrication due to preparation simplicity and good performance in ionic exchange measurements [9, 21].

This paper will focus on two AEMs (QAPSF-1 and QAPSF-2) prepared by a chemical modification method using PSF as the base polymerand trimethylamine (TMA) and N,N,N',N'-tetramethyl-1,6-hexanediamine (TMHDA) as the amination agents. TMHDA not only acts as an amination agent, but also because of the long alkyl chain, can be used as a crosslinker. The length of the alkyl group chain has a significant effect on the membrane conductivity. Applying a crosslinking agent with a short alkyl chain leads to lower ionic conductivity. This is due to the fact that a crosslinked structure with short alkyl chain provides smaller spaces for hydroxide ion transport. Therefore, a TMHDA with a long alkyl chain can be an appropriate crosslinker with larger spaces for hydroxide ion transfer and higher ionic conductivity values. Using this diamine simplifies the membrane preparation route by merging the crosslinking and functionalizing processes into one step [18, 21-23]. For membrane QAPSF-1 only TMA was used as an amination agent, and for membrane QAPSF-2 both TMA and TMHDA were used to investigate the role of TMHDA as an amination and crosslinking agent in the AEM performance. Degree of chloromethylation for chloromethylated PSF (CMPSF) was determined using $^1$HNMR spectra. Ion transport properties include ionic conductivity, ion exchange capacity (IEC) and ion transport activation energy, and the water content associated properties including water uptake (WU) and hydrated number were measured for the prepared QAPSF membranes. The obtained results showed that the AEM with the cross linked structure (QAPSF-2) had nearly similar ion transport properties with the membrane without a crosslinker (QAPSF-1). However, the dimensional stability and water content associated properties were improved significantly for the membrane utilizing the crosslinking agent.

## 2. Experimental

### 2.1. Materials

Polysulfone (PSF)- average $M_w$~35000, $M_n$~16000, chlorothrimethylsilane-98%,N,N,N',N'-tetramethyl-1, and 6-hexanediamine - 99% (TMHDA) were bought from Sigma-Aldrich. Chloroform, paraformaldehyde, N-methyl- 2-pyrrolidone (NMP), trimethylamine (TMA) - 40 wt% solution in $H_2O$, ethanol - 99%, potassium hydroxide (KOH) - 84%, sodium hydroxide (NaOH) - 99%, hydrochloric acid (HCl) - fuming 37%, and phenolphthalein - 1% solution in ethanol were supplied by Merck Chemicals. Stannic chloride ($SnCl_4$) was purchased from Scharlau. All chemicals were used without further purification.

### 2.2. AEM preparation

The AEM samples were prepared by a chemical modification method in three steps: chloromethylation, amination and alkalization as shown in Figure 1.

#### 2.2.1. Chloromethylation

The chloromethylation step was carried out based on a procedure adapted by Avram and co-workers [20]. 5g of PSF was dissolved in 250mL chloroform.

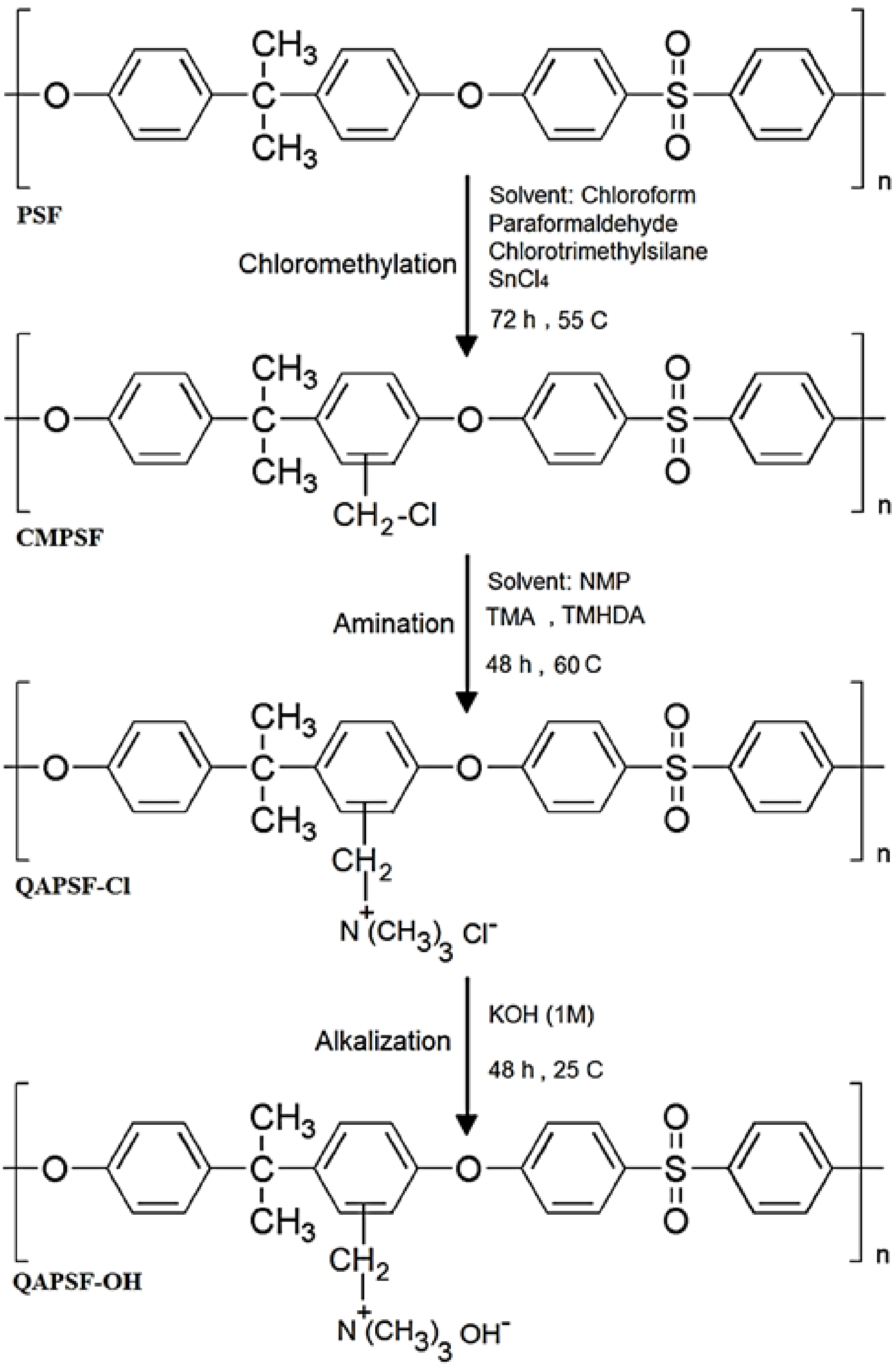

**Fig. 1. AEM preparation route based on quaternized PSF and ammonium groups**

Subsequently, the solution was transferred to three necked flasks equipped with a reflux condenser and magnetic stirrer. When the temperature of the mixture reached 55°C, 3.38g of paraformaldehyde and 12.3g of chlorotrimethylsilane were added to the mixture. Finally, $SnCl_4$ as the reaction catalyst was added drop wise to the solution. The chloromethylation reaction was carried out for 72h. The obtained solution from the chloromethylation reaction was precipitated in ethanol and vacuum filtrated to collect white solid particles of CMPSF. The obtained CMPSF was dried in a vacuum oven at 50°C for a day.

### 2.2.2. Amination

In this step 2g of CMPSF powder was dissolved in 20 mL NMP solvent. Next, 0.36cc of TMHDA and 2.82 cc of TMA were added to the mixture in order to obtain a molar ratio of 1:3:0.3 for $CH_2Cl$: TMA: TMHDA (TMHDA was only added in the QAPSF-2 or cross linked structure case). Amination reaction was carried out at 60°C for 48h. When the reaction was completed, the solution was degassed, casted on a glass plate and dried in a 60°C oven to remove solvent. To ensure that all solvent evaporated, the AEM film was vacuum dried at 80°C for 12h. The final product of this step was AEMs in chloride form (QAPSF-Cl) with an average thickness of 50-60 micron.

### 2.2.3. Alkalization

In the alkalization step the AEM films in chloride form were soaked in 1M KOH solution for 48 h at room temperature. The KOH solution was refreshed several times throughout this time to ensure the exchange of all chloride ions with hydroxide ones. The AEM films in hydroxide form (QAPSF-OH) were then washed and immersed in deionized water for 48 h to remove residual KOH.

## 2.3. Characterization of CMPSF and AEM

### 2.3.1. $^1$HNMR Spectra

The degree of chloromethylation (DC) of CMPSF was determined by proton NMR ($^1$HNMR) spectroscopy. The DC is the average number of chloromethylated groups per PSF monomer unit. The $^1$HNMR spectra were measured on a 400 MHz Bruker instrument using deuterated chloroform ($CDCl_3$) as solvent. The DC was calculated by integration of the peak area of chloromethyl ($CH_2Cl$) and isopropylidene ($C(CH_3)_2$) groups according to the following procedure and equation (4).

1) Each PSF monomer has 6 methyl protons; therefore, the peak area for a proton can be calculated by equation (1):

$$peak\ area\ for\ a\ proton = \frac{A_{C(CH_3)_2}}{6} \quad (1)$$

2) The number of $CH_2Cl$ group protons can be determined by equation (2):

$$number\ of\ CH_2Cl\ group\ protons = \frac{A_{CH_2Cl}}{peak\ area\ for\ a\ proton} \quad (2)$$

3) Each $CH_2Cl$ group on the PSF monomer has 2 protons; so finally, the number of $CH_2Cl$ groups for each PSF monomer (DC) can be calculated by equation (3):

$$DC = \frac{number\ of\ CH_2Cl\ group\ protons}{2} \quad (3)$$

4) By combining the mentioned equations, equation (4) can be derived as follows:

$$DC(\%) = \frac{number\ of\ CH_2Cl\ groups}{1\,PSF\ monomer} \times 100 = \frac{3 \times A_{CH_2Cl}}{A_{C(CH_3)_2}} \times 100 \quad (4)$$

where $A_{CH_2Cl}$ is the peak area of $CH_2Cl$ protons at 4.4-4.6 ppm and $A_{C(CH_3)_2}$ corresponds to the peak area of $C(CH_3)_2$ protons at 1.6-1.8 ppm in $^1$HNMR spectra.

### 2.3.2. ATR-FTIR spectra

The ATR-FTIR absorption spectra of CMPSF and prepared AEMs were recorded on Shimadzu FTIR-8400S in the spectral range of 500-4000 $cm^{-1}$.

### 2.3.3. Hydroxide conductivity and activation energy measurement

The Through plane ionic (hydroxide) conductivity was measured by electrochemical impedance spectroscopy (EIS) using Bio-Logic Science Instruments (SP-150 potentiostat). The EIS tests were performed at an oscillating voltage of 10mV and the frequency ranged from 1MHz to 10Hz. Before starting the measurements AEMs were kept in deionized water for 24h to minimize their exposure to ambient $CO_2$.

The membrane samples were taken out quickly and then sealed between two stainless steel electrodes. The conductivity was measured within the temperature range of 25 to 80 °C under 100% relative humidity (RH). The overall resistance (membrane resistance and stainless steel cell resistance) was determined from the intercept of the Nyquist plot at high frequency with a real impedance axis. Thus, the ionic conductivity can be calculated from the membrane resistance according to equations (5) and (6):

$$\sigma = \frac{l}{R_{mem} \times A} \tag{5}$$

$$R_{mem} = R_{overall} - R_{cell} \tag{6}$$

where $\sigma$ is the ionic conductivity (S/cm), $l$ is the membrane thickness (cm), $A$ is the membrane area (cm$^2$), $R_{overall}$ (Ω or 1/S) is the total resistance obtained from the Nyquist plot, $R_{cell}$ is the conductivity cell resistance (Ω or 1/S) and $R_{mem}$ is the membrane resistance (Ω or 1/S).

Furthermore, while the temperature dependency of hydroxide conductivity was governed by Arrhenius form, equation (7), apparent activation energy for ion transport was determined using a linear Arrhenius relationship between lnσ and 1000/T as shown in equation (8):

$$\sigma = \sigma_0 \exp\left(\frac{-E_a}{RT}\right) \tag{7}$$

$$E_a = -b \times R \tag{8}$$

where $\sigma_0$ is the pre-exponential factor, $E_a$ is the apparent activation energy (kJ/mol), $R$ is the gas constant (8.314 J/mol.K), $T$ is temperature (K) and $b$ is the slope of the linear regression of lnσ vs. 1000/T plots.

### 2.3.4. Ion exchange capacity measurement

The IEC (number of functional cationic sites per gram of dry membrane) was determined by back titration. The AEM samples were immersed in a 0.1M HCl solution for 24 h. Subsequently, the HCl solution was titrated with a 0.1M NaOH solution using phenolphthalein as an indicator. The IEC was calculated from equation (9):

$$IEC = \frac{M_1V_1 - M_2V_2}{m_{dry}} \tag{9}$$

where $M_1$ (M) and $V_1$ (mL) are the concentration and volume of the initial HCl solution, and $M_2$ (M) and $V_2$ (mL) are the concentration and volume of the NaOH solution used for titration, respectively. mdry (g) is the weight of the dry AEM sample.

### 2.3.5. Water uptake and hydrated number measurement

Water uptake (WU) was determined by measuring the weight difference between the wet and dry AEMs. The AEM samples in chloride (Cl$^-$) and hydroxide (OH$^-$) form were soaked in deionized water for 48 h at room temperature. Then the membranes were taken out, the surface water was wiped away, and the weight of the membrane was measured ($W_{wet}$). After that the membranes were dried under vacuum at 60°C for a day and their weight was recorded ($W_{dry}$). The WU for the AEMs was determined from equations (10):

$$WU(\%) = \frac{W_{wet} - W_{dry}}{W_{dry}} \times 100 \tag{10}$$

The hydrated number ($\lambda$) which is the number of water molecules per quaternized groups can be calculated from WU and IEC according to the following equation [26]:

$$\lambda = \frac{WU}{18.02} \times \frac{1000}{IEC} \tag{11}$$

### 2.3.6. Alkaline stability measurements

The alkaline stability of the prepared AEMs was evaluated by ionic conductivity. The membrane samples were exposed to a 3M KOH solution at 60°C for 50 h. After the treatment the membrane samples were washed with deionized water several times until neutralization. The ionic conductivity of the membranes after alkaline treatment was measured at 25°C and 60°C. Relative loss of ionic conductivity was calculated by equation (12):

$$Relative\,loss(\%) = \frac{\sigma_1 - \sigma_2}{\sigma_1} \times 100 \qquad (12)$$

where $\sigma_1$ (mS/cm) and $\sigma_2$ (mS/cm) are the ionic conductivity values before and after alkaline treatment, respectively.

## 3. Results and discussion

### 3.1. Synthesis of CMPSF and $^1$HNMR spectra study

The conventional method for chloromethylation is performed by chloromethyl methyl ether (CMME) which is carcinogenic and harmful to both humans and the environment. Therefore, in this study the chloromethylation step was carried out based on a route reported by Avram and co-workers. The chloromethylation of PSF was confirmed by the $^1$HNMR spectra. In Figure 2, the $^1$HNMR spectrum of CMPSF is illustrated. As clearly seen in this figure, the CMPSF shows a peak at 4.4-4.6 ppm which is assigned to the hydrogen proton of chloromethyl groups ($-CH_2C_l$). According to the equation (4), the CMPSF has a DC(%) value of 143%.

### 3.2. Preparation of AEMs based on QAPSF

Two different AEM samples, denoted as QAPSF-1 and QAPSF-2, were prepared by chemical modification according to Table 1. QAPSF-1 was prepared with only TMA as an amination agent while QAPSF-2 was prepared with TMA and TMHDA as amination and crosslinking agents. The cross linked structure of the QAPSF-2 membrane is shown in Figure 3. Figure 4

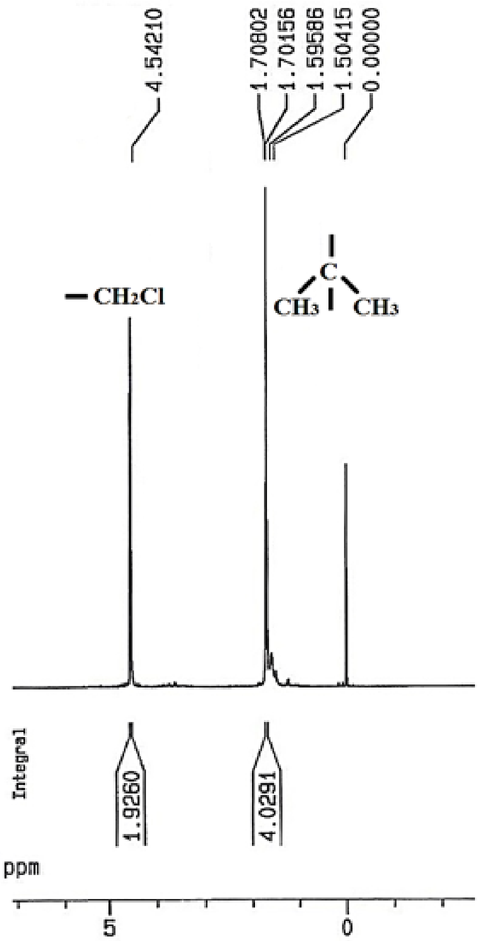

**Fig. 2. $^1$HNMR spectra for CMPSF.**

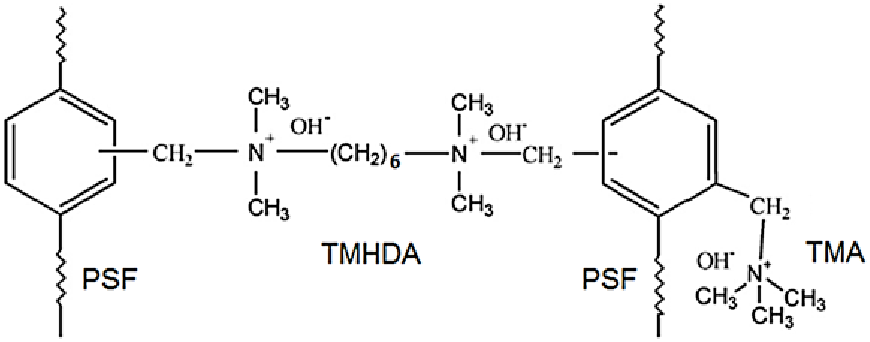

**Fig. 3. TMHDA acts as amination and crosslinking agent between two PSF chains.**

**Table 1. Chloromethylation and amination conditions used for AEM preparation**

| | Chloromethylation | | | Amination | | |
|---|---|---|---|---|---|---|
| membrane | time (h) | temperature (°C) | DC (%) | time (h) | temperature (°C) | $CH_2Cl$:TMA:TMHDA (molar ratio) |
| QAPSF-1 | 72 | 55 | 143 | 48 | 60 | 1:3:0 |
| QAPSF-2 | 72 | 55 | 143 | 48 | 60 | 1:3:0.3 |

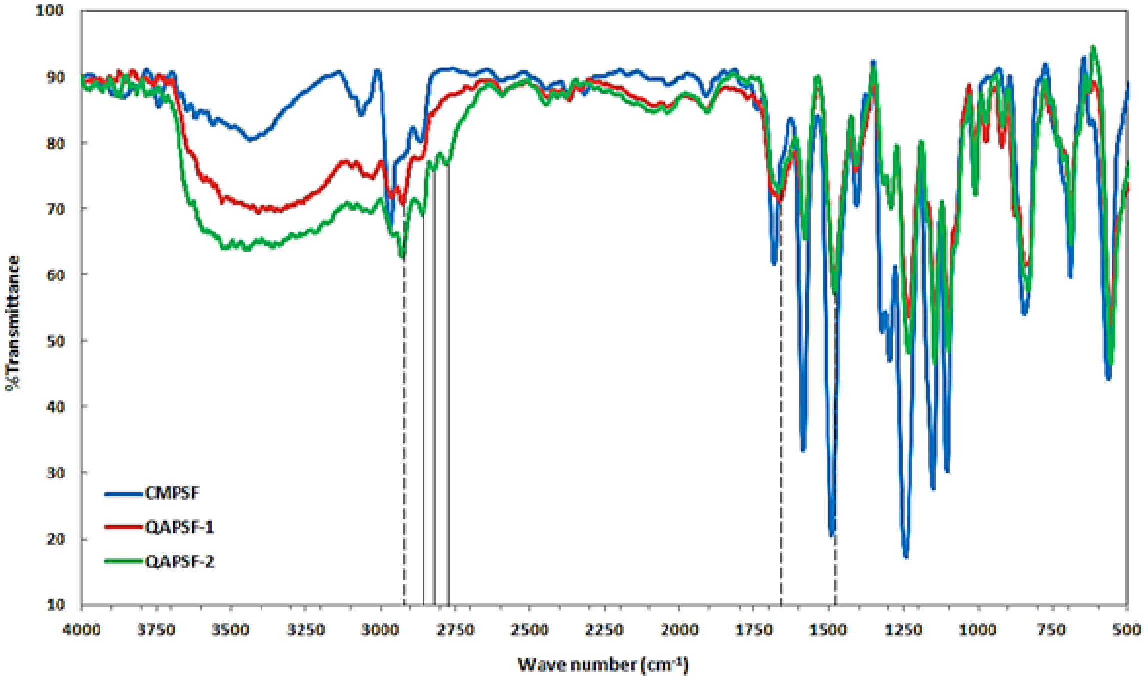

**Fig. 4. ATR-FTIR spectra for CMPPSF,QAPSF-1 and QAPSF-2.**

shows the ATR-FTIR spectra for CMPSF, QAPSF-1 and QAPSF-2. As seen in this figure, for the QAPSF-1 membrane the peaks at 2964 $cm^{-1}$, 1646 $cm^{-1}$ and 1475 $cm^{-1}$ (dash lines) are attributed to the stretching vibration of quaternary ammonium groups that show successful amination reaction. For the QAPSF-2 membrane the peaks at 2862 $cm^{-1}$, 2825 $cm^{-1}$ and 2786 $cm^{-1}$ (straight lines) are attributed to the stretching vibration of $–CH_2$- coming from the crosslinked structure. The QAPSF-2 had similar peaks with QAPSF-1 because of a TMA presence in the membrane structure. These data are in accordance with other literature [17, 18, 27].

### 3.3. Hydroxide conductivity, activation energy and IEC for AEMs

Hydroxide conductivity values at 25-80°C were calculated using resistance obtained from the Nyquist plot. Table 2 summarizes the membrane resistance at different temperatures for the prepared AEMs. Furthermore, Table 3 reports the ionic conductivity, IEC, and activation energy for QAPSF-1 and QAPSF-2. As can be seen, by increasing the temperature the membrane resistance values were decreased, the ionic conductivity values were improved, and finally, lower values of activation energy resulted. Obviously, as the temperature increases, the free volume expands and the anion transferring channels become wider, which

**Table 2. AEMs resistance calculated from Nyquist plot at different temperatures**

| membrane | σ (mS/cm) at 25 °C | σ (mS/cm) at 40 °C | σ (mS/cm) at 60 °C | σ (mS/cm) at 80 °C | IEC (meq/gr) | $E_a$ (kJ/mol) |
|---|---|---|---|---|---|---|
| QAPSF-1 | 11.90 | 17.24 | 22.73 | 26.32 | 1.43 | 12.88 |
| QAPSF-2 | 11.54 | 16.66 | 22.22 | 26.09 | 1.24 | 12.78 |

**Table 3. Ionic conductivity, IEC and activation energy of prepared AEMs**

| membrane | thickness (micron) | $R_{mem}$ (Ω) at 25 °C | $R_{mem}$ (Ω) at 40 °C | $R_{mem}$ (Ω) at 60 °C | $R_{mem}$ (Ω) at 80 °C |
|---|---|---|---|---|---|
| QAPSF-1 | 50 | 0.42 | 0.29 | 0.22 | 0.19 |
| QAPSF-2 | 60 | 0.52 | 0.36 | 0.27 | 0.23 |

improves overall mobility of ions and polymer chains, and consequently the ionic conductivity increases [28]. In addition by decreasing the energy barrier for ion transport through the polymer, the ionic conductivity through the AEM increases. As presented in Table 3, QAPSF-2 with the crosslinker had nearly similar values of ion conductivity and activation energy. This fact shows that the TMHDA as an amination agent and crosslinker does not inversely affect the membrane ion transport properties. Figure 5 presents the Nyquist plot for QAPSF-2 at 80 °C. The overall resistance (membrane resistance and conductivity cell resistance) was determined from the intercept of the Nyquist plot with the real impedance axis.

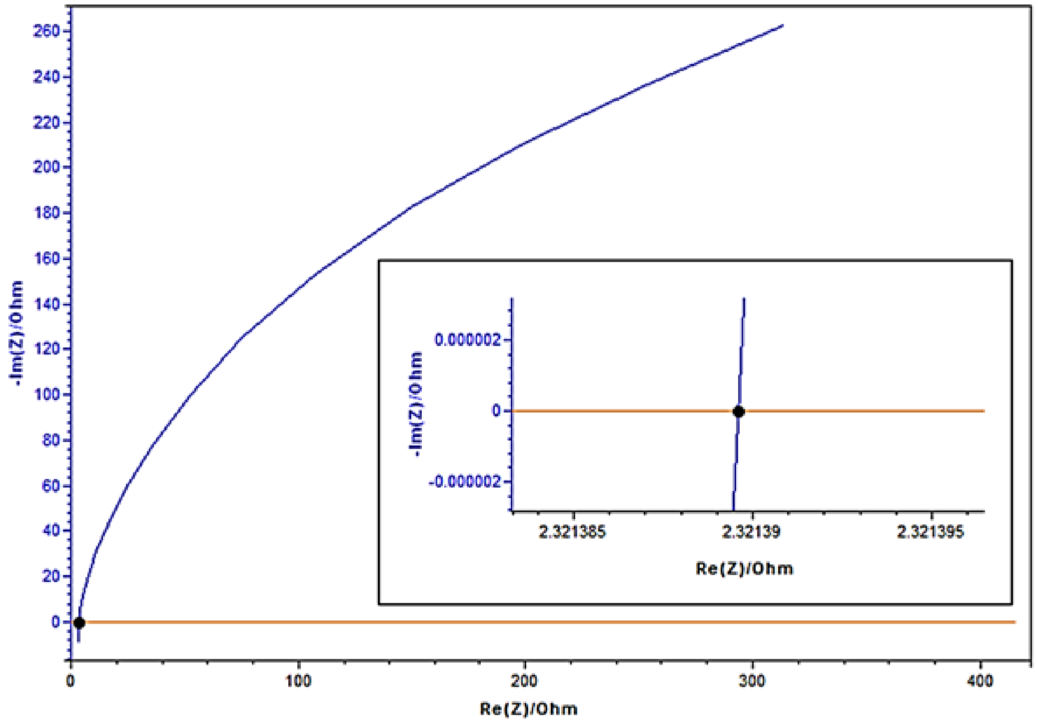

Fig. 5. Nyquist plot and related overall resistance of QAPSF-2 at 80 °C.

**Table 4.WU and hydrated number of the prepared AEMs in chloride and hydroxide forms**

| membrane | WU(%) $OH^-$ form | WU(%) $Cl^-$ form | λ $OH^-$ form | λ $Cl^-$ form |
|---|---|---|---|---|
| QAPSF-1 | 122.81 | 33.83 | 47.83 | 13.17 |
| QAPSF-2 | 93.98 | 22.53 | 41.99 | 11.41 |

### 3.4. Water uptake and hydrated number for AEMs

The water content associated properties of the prepared AEMs including the WU and hydrated number for both chloride and hydroxide forms are reported in Table 4. Generally, these parameters values will increase with the enhancement of IEC for AEMs. A higher IEC makes the ionic clusters larger and hydrophilic channels more continuous which in turn expands the overall hydrophilic domains and consequently improves water content associated properties [8, 29]. As presented in this table, the WU and hydrated number values of the AEMs in hydroxide form was greater than the values of the AEMs in chloride form. This phenomenon can be attributed to the coordination number of hydroxide ion in a water molecules network. Each hydroxide ion is surrounded by four water molecules, therefore the AEMs in hydroxide form uptakes more water molecules compared with AEMs in chloride form [2, 30]. As reported in Table 4, the water absorption for the QAPSF-2 membrane with TMHDA as a crosslinker was controlled and this membrane had more improved dimensional stability compared with QAPSF-1.

### 3.5. Alkaline stability experiments

The alkaline stability experiments were performed for both QAPSF-1 and QAPSF-2 membranes by treatment with a 3M KOH solution at 60°C for 50h. After treatment, QAPSF-1 did not show good stability and became very brittle, thus the ionic conductivity test could not be performed for this membrane. However, the QAPSF-2 showed good stability according to Figure 6. This figure represents the ionic conductivity of the QAPSF-2 membrane at 25°C and 60°C, before and after treatment with the KOH solution. As seen, the ionic conductivity decreased with a relative loss of 65% and 62% at 25°C and 60°C, respectively. The alkaline stability of QAPSF-2 is due to the fact that the TMHDA as a crosslinker strengths the membrane structure and decelerated the degradation process. The AEM degradation occurred by Hofmann elimination and nucleophilic substitution as shown in Figure 7.

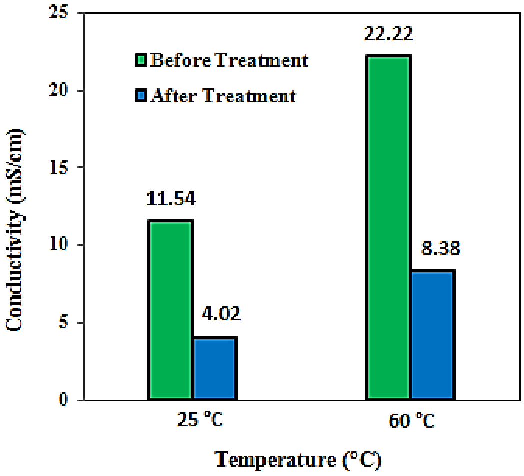

**Fig. 6. Ionic conductivity of QAPSF-2 at 25°C and 60°C before and after alkaline treatment.**

### 3.6. Comparison of Present Study with Literature

A comparison between data published in the literature and the data obtained in this study is presented in Table 5. As observed, the performance of the AEMs which were prepared in this study is in good agreement with other researchers.

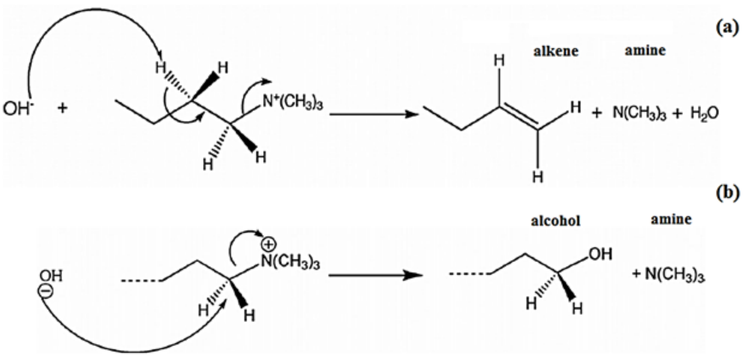

**Fig. 7. Degradation of ammonium groups in alkaline media by (a) Hofmann elimination and (b) nucleophilic substitution**

**Table 5. Comparison of experimental data with published data for AEMs based on PSF and ammonium groups**

| AEM | Amine group | σ (mS/cm) | IEC (meq/gr) | WU or SR (%) | λ or $E_a$ (kJ/mol) | Ref. |
|---|---|---|---|---|---|---|
| PSF-TMA$^+$-OH | TMA | 17-32<br>(30-70°C) | 2.05 | WU=200 (30°C) | - | [31] |
| QPSF | TMA- TMHDA | 11 (25°C) | - | SR= 37<br>(25°C) | - | [27] |
| QAPS-OH | TMA | 18-34<br>(20-80°C) | 1.18 | WU= 230 | - | [23] |
| xQAPS-PTFE | TMA | 35 (60°C) | 1.23 | SR= 3<br>(60°C) | - | [32] |
| QAPS-PTFE | TMA | 12-27<br>(20-70°C) | 1.27 | WU= 55 (30°C) | - | [11] |
| PSF-C1 | TMA | 13-27<br>(25-60°C) | 3 | - | - | [33] |
| DAPSF | TMA -TMHDA | 9-28<br>(30-80°C) | 0.91 | SR=10<br>(30°C) | - | [18] |
| QPSF/$TiO_2$10% | TMA-$TiO_2$ | 12 (21°C) | - | WU=39 | - | [5] |
| QPSU/$ZrO_2$10% | TMA | 15 | 0.92 | WU=19 | - | [19] |
| QAPSF-1 | TMA | 12-27<br>(25-80°C) | 1.43 | WU=122.81<br>(25°C) | λ=47.83<br>$E_a$=12.88 | This work |
| QAPSF-2 | TMA -TMHDA | 11-26<br>(25-80°C) | 1.24 | WU=93.98<br>(25 °C) | λ=47.83<br>$E_a$=12.78 | This work |

## 4. Conclusions

AEMs based on quaternized polysulfone containing ammonium groups (QAPSF) were prepared by a chemical modification method using chloromethylation, amination and alkalization. In the amination step, TMHDA was used as both an amination and crosslinking agent. The properties of the resulting membranes including ionic conductivity, IEC, activation energy for ion transport, and the WU and hydrated number were measured. The experiments results showed the membrane with the crosslinking agent (QAPSF-2) shows ion transport properties nearly similar to the membrane without the crosslinker (QAPSF-1). Although, QAPSF-2 has more improved water content associated properties and acceptable dimensional stability compared with QAPSF-1. Clearly by increasing the ionic conductivity and IEC values, WU and hydrated number will increase. Therefore, there is a trade-off between the ion transport properties and water content associated properties of the AEMs and both factors should be taken into consideration to obtain membranes with better performance. According to the ionic transport measurements and water content characterizations, the prepared QAPSF AEMs can be denoted as good candidates for SAFC application.

## 5. References

[1] Couture G, Alaaeddine A, Boschet F, Ameduri B. Polymeric materials as anion-exchange membranes for alkaline fuel cells. Progress in Polymer Science. 2011;36:1521-57.

[2] Merle G, Wessling M, Nijmeijer K. Anion exchange membranes for alkaline fuel cells: A review. Journal of Membrane Science. 2011;377:1-35.

[3] Wang Y-J, Qiao J, Baker R, Zhang J. Alkaline polymer electrolyte membranes for fuel cell applications. Chemical Society Reviews. 2013;42:5768-87.

[4] Zeng R, R. Varcoe J. Alkaline Anion Exchange Membranes for Fuel Cells- A Patent Review. Recent Patents on Chemical Engineering. 2011;4:93-115.

[5] Nonjola PT, Mathe MK, Modibedi RM. Chemical modification of polysulfone: Composite anionic exchange membrane with $TiO_2$ nano-particles. International Journal of Hydrogen Energy. 2013;38:5115-21.

[6] Gopi KH, Peera SG, Bhat SD, Sridhar P, Pitchumani S. Preparation and characterization of quaternary ammonium functionalized poly(2,6-dimethyl-1,4-phenylene oxide) as anion exchange membrane for alkaline polymer electrolyte fuel cells. International Journal of Hydrogen Energy. 2014;39:2659-68.

[7] Liu L, Li Q, Dai J, Wang H, Jin B, Bai R. A facile strategy for the synthesis of guanidinium-functionalized polymer as alkaline anion exchange membrane with improved alkaline stability. Journal of Membrane Science. 2014;453:52-60.

[8] Yan X, Gu S, He G, Wu X, Zheng W, Ruan X. Quaternary phosphonium-functionalized poly(ether ether ketone) as highly conductive and alkali-stable hydroxide exchange membrane for fuel cells. Journal of Membrane Science. 2014;466:220-8.

[9] Yan X, Wang Y, He G, Hu Z, Wu X, Du L. Hydroxide exchange composite membrane based on soluble quaternized polyetherimide for potential applications in fuel cells. International Journal of Hydrogen Energy. 2013;38:7964-72.

[10] Lu W, Shao Z-G, Zhang G, Zhao Y, Yi B. Crosslinked poly(vinylbenzyl chloride) with a macromolecular crosslinker for anion exchange membrane fuel cells. Journal of Power Sources. 2014;248:905-14.

[11] Zhao Y, Pan J, Yu H, Yang D, Li J, Zhuang L, et al. Quaternary ammonia polysulfone-PTFE composite alkaline anion exchange membrane for fuel cells application. International Journal of Hydrogen Energy. 2013;38:1983-7.

[12] Mabrouk W, Ogier L, Vidal S, Sollogoub C, Matoussi F, Fauvarque JF. Ion exchange membranes based upon crosslinked sulfonated polyethersulfone for electrochemical applications. Journal of Membrane Science. 2014;452:263-70.

[13] Roddecha S, Dong Z, Wu Y, Anthamatten M. Mechanical properties and ionic conductivity of electrospun quaternary ammonium ionomers. Journal of Membrane Science. 2012;389:478-85.

[14] Abuin GC, Nonjola P, Franceschini EA, Izraelevitch FH, Mathe MK, Corti HR. Characterization of an anionic-exchange membranes for direct methanol alkaline fuel cells. International Journal of Hydrogen Energy. 2010;35:5849-54.

[15] Arges CG, Ramani V, Pintauro PN. Anion exchange membrane. Electrochemical Society Interface. 2010:31-5.

[16] Wang G, Weng Y, Chu D, Chen R, Xie D. Developing a polysulfone-based alkaline anion exchange membrane for

improved ionic conductivity. Journal of Membrane Science. 2009;332:63-8.

[17] Pantamas N, Khonkeng C, Krachodnok S, Chaisena A. Ecofriendly and Simplified Synthetic Route for Polysulfone-based Solid-State Alkaline Electrolyte Membrane. American Journal of Applied Sciences. 2012;9:1577.

[18] Zeng L, Zhao TS. High-performance alkaline ionomer for alkaline exchange membrane fuel cells. Electrochemistry Communications. 2013;34:278-81.

[19] Vinodh R, Purushothaman M, Sangeetha D. Novel quaternized polysulfone/$ZrO_2$ composite membranes for solid alkaline fuel cell applications. International Journal of Hydrogen Energy. 2011;36:7291-302.

[20] Avram E, Butuc E, Luca C, Druta I. Polymers with Pendant Functional Group. III. Polysulfones Containing Viologen Group. Journal of Macromolecular Science, Part A. 1997;34:1701-14.

[21] Zhang S, Li C, Xie X, Zhang F. Novel cross-linked anion exchange membranes with diamines as ionic exchange functional groups and crosslinking groups. International Journal of Hydrogen Energy. 2014;39:13718-24.

[22] Wang W, Wang S, Li W, Xie X, lv Y. Synthesis and characterization of a fluorinated cross-linked anion exchange membrane. International Journal of Hydrogen Energy. 2013;38:11045-52.

[23] Park J-S, Park S-H, Yim S-D, Yoon Y-G, Lee W-Y, Kim C-S. Performance of solid alkaline fuel cells employing anion-exchange membranes. Journal of Power Sources. 2008;178:620-6.

[24] Pan J, Lu S, Li Y, Huang A, Zhuang L, Lu J. High-Performance Alkaline Polymer Electrolyte for Fuel Cell Applications. Advanced Functional Materials. 2010;20:312-9.

[25] Roddecha S, Dong Z, Wu Y, Anthamatten M. Mechanical properties and ionic conductivity of electrospun quaternary ammonium ionomers. Journal of Membrane Science. 2012;389:478-85.

[26] Qiao J, Fu J, Liu L, Liu Y, Sheng J. Highly stable hydroxyl anion conducting membranes poly (vinyl alcohol)/poly (acrylamide-co-diallyldimethylammonium chloride)(PVA/PAADDA) for alkaline fuel cells: Effect of cross-linking. international journal of hydrogen energy. 2012;37:4580-9.

[27] Wang X, Li M, Golding BT, Sadeghi M, Cao Y, Yu EH, et al. A polytetrafluoroethylene-quaternary 1,4-diazabicyclo-[2.2.2]-octane polysulfone composite membrane for alkaline anion exchange membrane fuel cells. International Journal of Hydrogen Energy. 2011;36:10022-6.

[28] Li X, Wang L, Cheng S. Investigation on structure and properties of anion exchange membranes based on tetramethylbiphenol moieties containing copoly(arylene ether)s. Journal of Applied Polymer Science. 2015;132:n/a-n/a.

[29] Jheng L-c, Hsu SL-c, Lin B-y, Hsu Y-l. Quaternized polybenzimidazoles with imidazolium cation moieties for anion exchange membrane fuel cells. Journal of Membrane Science. 2014;460:160-70.

[30] Li X, Yu Y, Liu Q, Meng Y. Synthesis and characterization of anion exchange membranes based on poly (arylene ether sulfone)s containing various cations functioned tetraphenyl methane moieties. international journal of hydrogen energy. 2013;38:11067-73.

[31] Arges CG, Parrondo J, Johnson G, Nadhan A, Ramani V. Assessing the influence of different cation chemistries on ionic conductivity and alkaline stability of anion exchange membranes. Journal of Materials Chemistry. 2012;22:3733-44.

[32] Li G, Pan J, Han J, Chen C, Lu J, Zhuang L. Ultrathin composite membrane of alkaline polymer electrolyte for fuel cell applications. Journal of Materials Chemistry A. 2013;1:12497-502.

[33] Jung H, Fujii K, Tamaki T, Ohashi H, Ito T, Yamaguchi T. Low fuel crossover anion exchange pore-filling membrane for solid-state alkaline fuel cells. Journal of Membrane Science. 2011;373:107-11.